Contents lists available at ScienceDirect

Brain, Behavior, & Immunity - Health

Elevated matrix Metalloproteinase-9 associated with reduced cerebellar perineuronal nets in female mice with toxoplasmosis

Jianchun Xiao [*], Jing Huang, Robert H. Yolken

Stanley Division of Developmental Neurovirology, Department of Pediatrics, Johns Hopkins School of Medicine, Baltimore, MD, 21287, USA

A B S T R A C T

Brain infection by the parasite *Toxoplasma gondii* is thought to impair learning and memory, although the underlying mechanisms remain largely unknown. Recent studies suggest that perineuronal nets (PNNs) and their key regulator, matrix metalloproteinase-9 (MMP-9), have essential roles in synaptic plasticity associated with learning and memory. We investigated their roles in a chronic toxoplasmosis model using female mice. In mice with a high parasite burden of chronic infection, we found that MMP-9 expression was increased in the peripheral circulation and the brain. A correlation was found between the serum levels of MMP-9 and antibodies to the *Toxoplasma* matrix antigen MAG1, a surrogate marker for *Toxoplasma* tissue cysts in the brain. MMP-9 elevation was accompanied by increased expression of its endogenous regulators, TIMP-1 and NGAL. An increase in the levels of GSK-3α/β was observed, alongside a decrease in inhibitory GSK-3α/β (Ser-21/Ser-9) phosphorylation. MMP-9 expression was notably associated with the loss of PNNs but increased expression of the synaptic vesicle protein synaptophysin. There was a trend toward a negative correlation between MMP-9 and aggrecan expression, a critical PNN component. Together, these results suggest that chronic *Toxoplasma* infection can cause an increase in MMP-9 expression, resulting in the degradation of PNNs, which provides a possible mechanism for *Toxoplasma*-associated deficits in learning and memory.

1. Introduction

The brain's extracellular matrix (ECM) acts as a dynamic scaffold for cells and is a reservoir of signaling molecules (Nicholson and Sykova, 1998). Perineuronal nets (PNNs) are specialized ECM structures that condense around the soma and proximal dendrites of subpopulations of neurons in various brain regions, including the forebrain, midbrain, and cerebellum (Bertolotto et al., 1996). Owing to their unique structural organization, PNNs have neuroprotective capacities but also participate in signal transduction and controlling neuronal activity and plasticity (Testa et al., 2019). Mounting evidence supports a critical role for PNNs in normal brain function, such as learning and memory, and in many brain disorders, such as schizophrenia, Alzheimer's disease, epilepsy, and autism (Sorg et al., 2016; Wen et al., 2018b). PNNs are made of chondroitin sulfate proteoglycans (CSPGs), which include aggrecan, brevican, neurocan, and versican. Aggrecan is the key component for assembling and sustaining the PNNs structure and function (Giamanco et al., 2010; Rowlands et al., 2018). Studies demonstrated that loss of PNNs by aggrecan removal reopens juvenile plasticity in visual cortex

and affects memory processing (Rowlands et al., 2018).

Matrix metalloproteinases (MMPs) are the principal ECM-degrading enzymes. One of the MMPs, MMP-9, has been suggested to degrade CSPGs (Pollock et al., 2014). Elevated levels of MMP-9 associated with reduced PNNs have been found in mouse models of Fragile X Syndrome and post-mortem brain tissues of patients with multiple sclerosis (Gray et al., 2008; Wen et al., 2018a). Generally, the activity of MMP-9 is strictly controlled temporally and spatially at several levels, including enzyme activation, inhibition, complex formation, and compartmentalization (Dzwonek et al., 2004). MMP-9 is initially synthesized as inactive proenzymes and later converted to active forms by propeptide processing. The formation of different MMP-9 complexes results in altered biochemical properties of the enzyme. When tissue inhibitor of metalloproteinase (TIMP-1) binds to MMP-9, it inhibits its proteolytic activity. Conversely, when neutrophil gelatinase-associated lipocalin (NGAL) forms a complex with MMP-9, it increases the stability of the enzyme. MMP-9 is usually located in the hippocampus, cerebellum, and cerebral cortex, but its expression in the naive brain is low or absent (Dzwonek et al., 2004). Studies have shown increased expression of

MMP-9 during tissue remodeling events, such as wound healing, tumor invasion, neurogenesis, axonal growth, angiogenesis, CNS barrier disruption, myelinogenesis, and demyelination (Brkic et al., 2015). In addition, infections caused by bacteria, viruses, and parasites have been found to impact MMP-9 expression (Bruschi and Pinto, 2013; Vafadari et al., 2016). For example, high levels of MMP-9 were found in the cerebrospinal fluid of patients with bacterial meningitis (Leppert et al., 2000) and in the serum of infants with HHV-6 infection (Kittaka et al., 2014). Glycogen synthase kinase 3 (GSK-3), a key player in multiple cells signaling pathways, has been found to cooperate with MMP-9 in controlling dendritic spine morphology (Kondratiuk et al., 2017).

Toxoplasma gondii is a single-celled and obligatory intracellular parasite that can affect most warm-blooded animals, including mice and humans. It causes neurological abnormalities in some immune-compromised individuals and babies born to mothers infected with *Toxoplasma* during pregnancy. *Toxoplasma* infection may also increase the risk of multiple brain disorders in immune-competent individuals, including depression, schizophrenia, Parkinson's disease, and cognitive decline in the elderly (Xiao et al., 2018b, 2022). Studies conducted on mice have shown that infection with *Toxoplasma* impairs their learning and memory (Kannan and Pletnikov, 2012). Proposed hypotheses on the brain effects of *Toxoplasma* infection include increased levels of glutamate, reduced dendritic complexity and spine density, neural degeneration, and decreased expression of synaptic markers (David et al., 2016; Li et al., 2018, 2019; Parlog et al., 2014). It is unclear whether PNNs or MMP-9 are involved in *Toxoplasma*-related neuropathology. Previously, in vitro studies have revealed that astroglia infected with *Toxoplasma* tachyzoites exhibit elevated levels of MMP-9 (Lu and Lai, 2013). In addition, increased levels of MMP-9 secretion were observed in the serum of pregnant women and umbilical cord blood from their offspring with *Toxoplasma* infection (Spann et al., 2017).

In the presented study, we investigated the expression of MMP-9, its complexes, and PNN integrity in a murine model of chronic toxoplasmosis. The cerebellum impacts various motor, cognitive, and emotional processes and has been implicated in numerous psychiatric disorders (Phillips et al., 2015). Recently, cerebellar plasticity and associative memories have been found to be controlled by PNNs (Carulli et al., 2020). As the cerebellum is a common site for both MMP-9 and PNN expression, we focused our investigation on this brain region. Our results revealed that mice with a high parasite burden exhibited increased MMP-9 expression and disruption of the PNN; those changes potentially contribute to the learning and memory deficiencies associated with *Toxoplasma* infections.

2. Materials and methods

Chronic mouse model of *Toxoplasma* infection. All mouse specimens were collected as part of a previously published study (Xiao et al., 2016); no additional animals were sacrificed for the present study. Animal protocols were reviewed and approved by the Animal Care and Use Committee of Johns Hopkins University. As described before (Xiao et al., 2016), 7- to 9-week-old female outbred CD-1 mice (ICR-Harlan Sprague) were infected intraperitoneally (i.p.) with 500 tachyzoites of *Toxoplasma* GT1 strain (type I, virulent). Control mice received vehicle only (PBS). The female mice were chosen for study because they tend to be less aggressive. To control tachyzoite proliferation and avoid animal death, infected mice, including controls, were treated with anti-*Toxoplasma* chemotherapy (sulfadiazine sodium) in drinking water (400 mg/liter; Sigma) from days 5–30. This model generates varied outcomes ranging from aborted to severe infections, closely resembling the heterogeneous effects of *Toxoplasma* exposure in humans (Xiao et al., 2022). At five months postinfection, mice were anesthetized using a mixture of ketamine (100 mg/kg), xylazine (20 mg/kg), and acepromazine (10 mg/kg) before decapitation. For immunofluorescent staining, the harvested brain samples were fixed at 4 °C in 4 % PFA, 10 % sucrose, and 30 % sucrose dissolved in PBS. Paraffin embedding and sectioning were

carried out at the Johns Hopkins Oncology Tissue Service. For tissue dissection, cerebellum was rapidly dissected, placed into RNAlater Solution (Thermo Scientific), and stored at −80 °C.

Enzyme-linked Immunosorbent Assay. Upon sacrifice, mouse peripheral blood was drawn using cardiac puncture and centrifuged at $1000 \times g$ for 15 min after 30 min of clotting at room temperature. The serum was transferred, aliquoted, and stored at −80 °C until analysis. Anti-*Toxoplasma* antibodies were measured (1:100 dilution) using a commercial ELISA kit (IB19213, IBL America), modified as previously described (Xiao et al., 2016). Antibodies against *Toxoplasma* cyst antigen MAG1 (1:100 dilution) were determined using our previously developed MAG1 ELISA assay (Xiao et al., 2013, 2021). MMP-9 levels were determined (1:50 dilution) using a commercial ELISA kit (MMPT90, R&D/Fisher Scientific). Optical density was read on FilterMax™ F5 Multi-Mode Microplate Reader (Molecular Devices).

Western blot analysis. Total proteins were extracted from the mouse cerebellum using T-PER™ Tissue Protein Extraction Reagent (Thermo Scientific) added with Halt Protease and Phosphatase Inhibitor Cocktail (Thermo Scientific). Protein concentrations were measured using a BCA protein assay kit (Thermo Scientific). 10–30 μg of total protein were loaded on 4–20 % TGX protein gel (Bio-Rad) for electrophoresis under non-reducing or reducing conditions and transferred to PVDF membranes (Bio-Rad). The membranes were blocked with StartingBlock T20 (TBS) Blocking Buffer (Thermo Scientific) for 1 h at room temperature (RT), followed by incubation with primary antibodies at 4 °C overnight. Proteins were probed with primary antibodies for MMP-9 (polyclonal, AF909, 1: 800, R&D systems), NGAL (polyclonal, ab63929, 1:500, Abcam), TIMP-1 (polyclonal, AF980, 1:500, R&D systems), synaptophysin (monoclonal, ab8049, 1:500, Abcam), pGSK-3α/β (Ser21/9) (polyclonal, 9331, 1:1000 dilution; Cell Signaling Technology), GSK-3α/β (polyclonal, 5676, 1:1000 dilution, Cell Signaling Technology), aggrecan (polyclonal, AB1031, 1:1000, Sigma), and brevican (monoclonal, 610,894, 1:1000, BD Biosciences). Bands were visualized using enhanced chemiluminescence (SuperSignal West Femto Maximum Sensitivity Substrate, Thermo Scientific). For the MMP-9 probe blots under reducing conditions, the membrane was stripped and reprobed with an anti-TIMP-1 antibody. After probing with either aggrecan or brevican, the membranes were stripped and reprobed with an anti-MMP-9 antibody. To assess whether the proteins were loaded equally, all membranes were stripped and reprobed for β-actin (monoclonal, A5441, 1:5000; Sigma). Relative optical density was determined using ImageLab software (Bio-Rad).

Gel Zymography. For electrophoresis, 25 μg of total protein was loaded on Novex® 10 % Zymogram Plus (Gelatin) Protein gels (ZY00100BOX, Invitrogen). Gels were then renatured using Renaturing Buffer (Invitrogen) for 30 min at RT with gentle agitation and equilibrated in Developing Buffer (Invitrogen) for 30 min, followed by incubation in Developing Buffer at 37 °C for 66 h. After briefly rinsing with distilled water, gels were stained with SimplyBlue SafeStain (LC6060, Thermo Fisher). Images were analyzed using ImageLab software (Bio-Rad).

Immunofluorescence staining. Paraffin wax-embedded sections were cut at a thickness of 5 μm. Serial sections (3 mice per group; 5 sections per mouse) were treated in xylene and a graduated alcohol series and rinsed in distilled water. Antigen retrieval was performed with Antigen Retrieval Reagent-Basic (CTS013, R&D Systems) and heated at 92–95 °C for 10 min. Sections were blocked with BlockAid blocking buffer (B10710, Fisher Scientific) for 30 min at RT. Sections were stained overnight using the following primary antibodies: anti-MMP-9 antibody (polyclonal, ab38898, 1: 100, Abcam), anti-synaptophysin antibody (monoclonal, ab8049, 1:100, Abcam), and anti-WFA (B-1355-2, 1:100, Vector Laboratories). Double-fluorescence staining was performed for these markers in different combinations. Secondary antibodies were purchased from ThermoFisher Scientific. Finally, the sections were stained with DAPI (4′,6-diamidino-2-phenylindole; Sigma-Aldrich) and mounted with prolong diamond antifade

mountant (ThermoFisher Scientific). Images were visualized using an Olympus BX41 microscope and a reflected fluorescence system. A confocal laser microscope was used to characterize morphology or verify the co-localization. Colocalization analysis of immunofluorescence signals was performed using an ImageJ plugin (JACoP), with the threshold set automatically by Costes' method (Bolte and Cordelieres, 2006). The Pearson's correlation coefficient was calculated from eight representative images.

Statistical analysis. Differences between the two groups were analyzed by Student's t-test. For multiple groups, ANOVA with Bonferroni's multiple comparisons was applied. Correlation analysis was performed using Pearson's correlation coefficient. Statistical analyses were conducted in Graph-Pad Prism V9.2.0. Significance was denoted as a P of <0.05.

3. Results

3.1. Toxoplasma tissue cyst-associated elevation of serum MMP-9 levels

We measured the serum levels of MMP-9 in CD-1 mice infected with a virulent *Toxoplasma* type I strain. As previously described (Xiao et al., 2016), mice were stratified into five groups based on antibody profiles: (i) unexposed control mice (IgG-/MAG1-), (ii) *Toxoplasma*-exposed mice with a high MAG1 antibody level (IgG+/MAG1+high, MAG1 level ≥0.5, designated as MAG1-high); (iii) *Toxoplasma*-exposed mice with a low MAG1 antibody level (IgG+/MAG1+low, MAG1 level <0.5, designated as MAG1-low), (iv) *Toxoplasma*-exposed mice that did not develop MAG1 antibodies (IgG+/MAG1-, designated as MAG1-negative), and (v) *Toxoplasma*-exposed mice that did not develop an antibody response (IgG-/MAG1-, designated as IgG-negative). *Toxoplasma* IgG indicates exposure to the parasite, while MAG1 antibody serves as a serologic marker for cyst burden (Xiao et al., 2016, 2023). MAG1 is a protein abundantly expressed in the cyst wall surrounding the bradyzoites and within the cyst (Ferguson and Parmley, 2002). We found that serum MMP-9 levels were significantly higher in mice with high MAG1 antibody levels compared to the other groups (Fig. 1A, mean ± SD ng/mL: MAG1-high 217 ± 132, MAG1-low 30.0 ± 12.5, MAG1-negative 29.3 ±

12.4, IgG-negative 32.8 ± 13.0, control 30.0 ± 8.51; $F_{(4, 32)} = 14.69$, P < 0.0001; post-hoc P < 0.0001). A strong positive correlation (r = 0.98, P < 0.0001, Fig. 1B) was found between MMP-9 and MAG1 antibody levels in the mice with MAG1 antibodies.

3.2. Toxoplasma tissue cyst-associated elevation of cerebellar MMP-9, TIMP-1, and NGAL

A unique characteristic of MMP-9 is its ability to exist in monomeric and disulfide-bonded dimeric forms (Olson et al., 2000). However, some dimers formed with MMP-9 can only be detected in SDS/PAGE under non-reducing conditions. To investigate these dimers, we examined MMP-9 and related proteins under both reducing and non-reducing conditions.

Non-reducing Conditions. Two forms of MMP-9 were observed in blots with anti-MMP-9 antibodies in the mouse cerebellum. These forms had molecular weights of ~150 kDa and ~110 kDa (Fig. 2A). In rodents, the molecular mass of NGAL-conjugated MMP-9 was reported at 135 kDa (Park et al., 2009). We ascribed the higher band to MMP-9/TIMP-1 due to its proximity to 150 kDa. The molecular mass of lower band corresponded to murine MMP-9 monomer, which has been reported at 105–110 kDa (Ramsey et al., 2005). The expression of MMP-9/TIMP-1 and MMP-9/NGAL were individually seen when anti-TIMP-1 or anti-NGAL antibodies were used (Fig. 2A). The MMP-9 monomer and complexes were expressed significantly higher in MAG1-high mice than in MAG1-low or control mice, as shown in these blots (For blots with anti-MMP-9 antibodies, MMP-9/TIMP-1: $F_{(2, 6)} = 8.498$, P = 0.0178, post-hoc P = 0.0187; MMP-9 monomer: $F_{(2, 6)} = 3.698$, P = 0.0898; For blots with anti-TIMP-1 antibodies, MMP-9/TIMP-1: $F_{(2, 6)} = 17.56$, P = 0.0031, post-hoc P = 0.0033; For blots with anti-NGAL antibodies, $F_{(2, 6)} = 5.941$, P = 0.0378, post-hoc P = 0.0495). Moreover, the MMP-9/TIMP-1 complex also showed an increase in MAG1-low mice compared to controls when blotted with anti-TIMP-1 antibodies (post-hoc P = 0.0315). Under non-reducing conditions, no apparent bands correspond to monomers TIMP-1 or NGAL.

Reducing Conditions. Blots with anti-MMP-9, anti-TIMP-1, or anti-NGAL antibodies revealed bands corresponding to MMP-9 (~110 kDa),

A

B
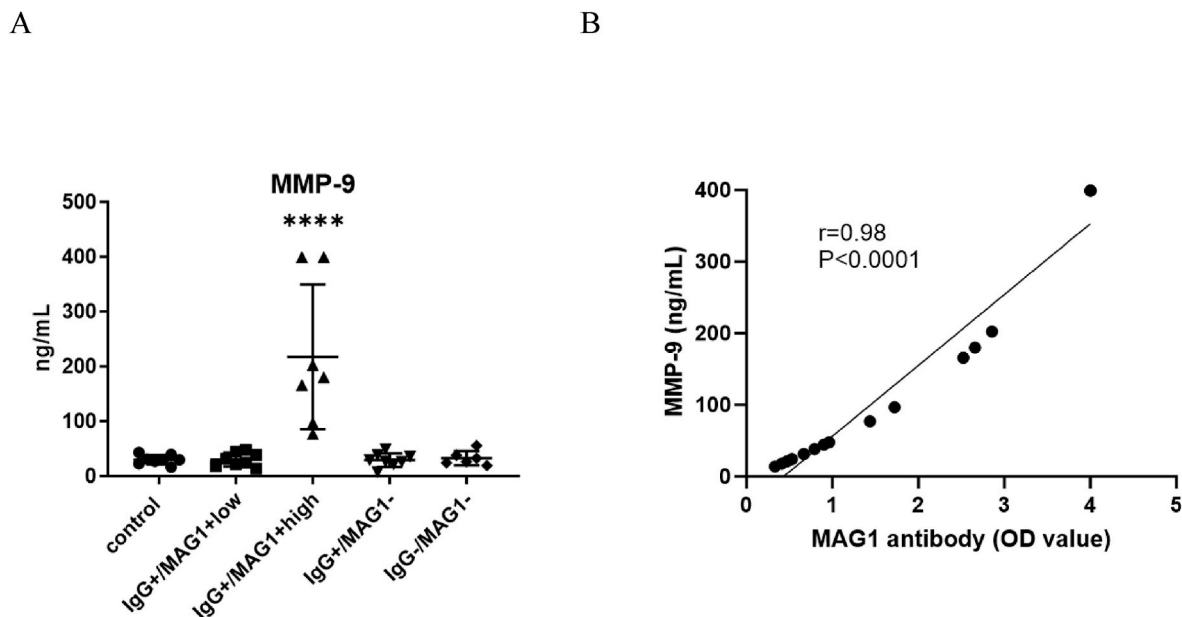
Fig. 1. Cyst-associated elevation of serum MMP-9 levels. Female CD-1 mice were infected intraperitoneally with 500 tachyzoites of GT1 strain and sacrificed at 5 months post-infection. (A) Distribution of MMP-9 concentration among the five groups stratified by antibody profiles. IgG indicates exposure to *Toxoplasma*, while MAG1 antibody serves as a serologic marker for cyst burden. Data are shown as mean ± SD, with individual values. (B) A strong positive correlation was found between MMP-9 and MAG1 antibody levels in mice with MAG1 antibodies, including the MAG1-high and MAG1-low groups. Statistically significant differences were determined by one-way ANOVA followed by Bonferroni's correction for multiple comparisons (A) or Pearson's correlation analysis (B). ****, P < 0.0001.

A

Non-reducing condition

B
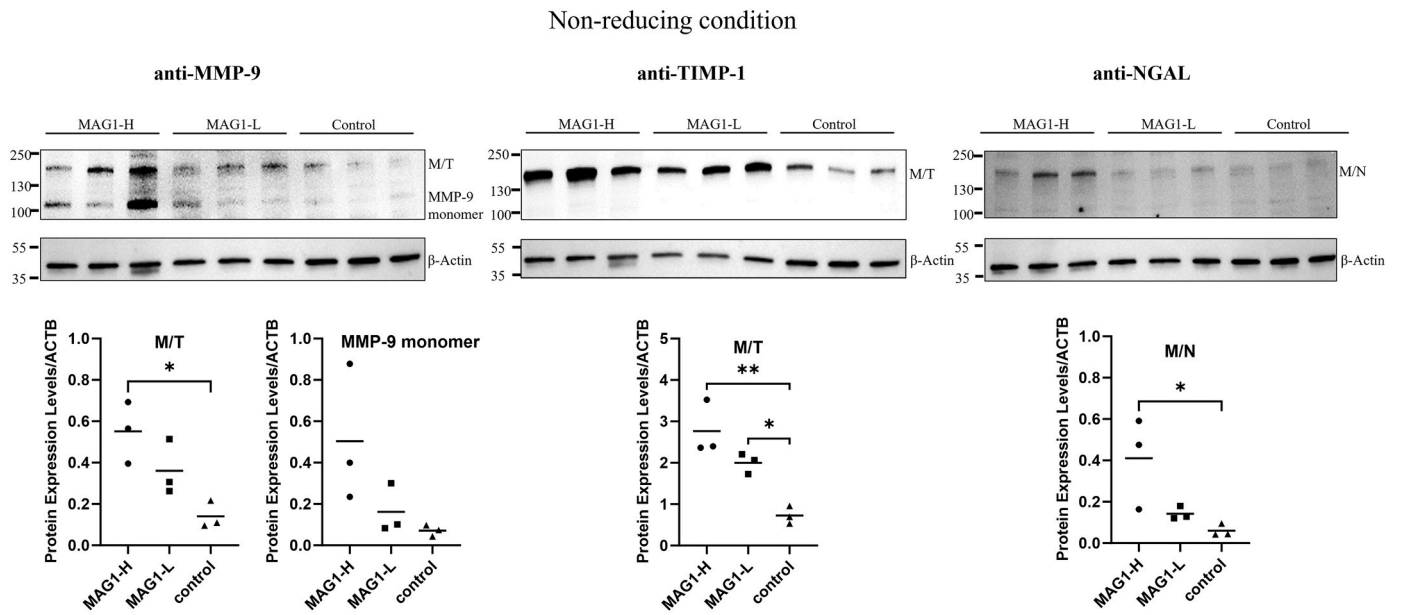
Reducing condition
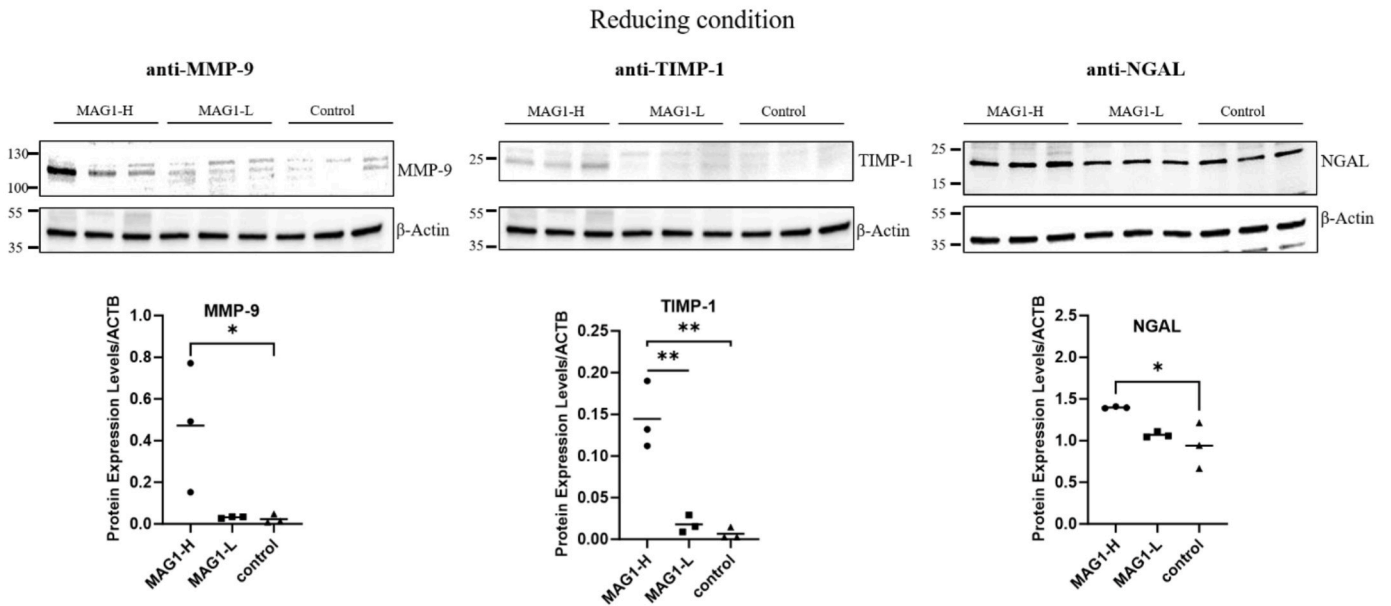
Fig. 2. Elevated expression of MMP-9, TIMP-1, and NGAL in the cerebellum of mice bearing a high burden of tissue cysts. The blot was probed with anti-MMP-9, anti-TIMP-1, and anti-NGAL antibodies under non-reducing (A) or reducing (B) conditions, among MAG1-high, MAG1-low, and control mice (n = 3 per group), alongside β-actin loading controls. Each data point and means obtained by densitometry analysis of blots were shown. A dagger indicates significant differences between experimental groups. *p < 0.05, **p < 0.01 (one-way ANOVA followed by Bonferroni's correction for multiple comparisons). M/T, MMP-9/TIMP-1 complex; M/N, MMP-9/NGAL complex.

TIMP-1 ($\sim$25 kDa), and NGAL ($\sim$23 kDa) monomers, respectively (Fig. 2B). The expression of these monomers was significantly higher in MAG1-high mice than that of MAG1-low or control groups (for MMP-9: $F_{(2, 6)} = 6.156$, $P = 0.0352$, post-hoc $P = 0.05$ vs control; for TIMP-1: $F_{(2, 6)} = 29.44$, $P = 0.0008$, post hoc $P = 0.0021$ vs MAG1-low, $P = 0.0014$ vs control; for NGAL: $F_{(2, 6)} = 6.513$, $P = 0.0314$, post hoc $P = 0.0384$ vs control).

3.3. Toxoplasma tissue cyst-associated elevation of the enzymatic level of MMP-9 monomer

Gel zymography is an activity-based assay that identifies MMPs by the degradation of their preferential substrate and by their molecular weight. It is important to note, however, that this assay detects both the latent and active forms of the MMPs that are being analyzed. As a result,

this assay can only measure the levels of MMPs but not their activity. Gelatin-substrate zymography is extensively used for the detection of MMP-2 and MMP-9 activity in biological samples. We detected two major clear bands against dark blue background, with molecular weights of ~110 kDa and ~68 kDa (Fig. 3). According to previous reports (Ramsey et al., 2005), the ~110 kDa bands corresponded to the MMP-9 monomer, and the ~68 kDa bands represented MMP-2. MMP-2 is an MMP housekeeping gene due to its high constitutive activity (DeLeon-Pennell et al., 2017). Thus, the expression of MMP-9 monomer was normalized to the corresponding values of MMP-2. We found that the enzymatic level of MMP-9 monomer was significantly higher in MAG1-high mice than in MAG1-low or control mice ($F_{(2, 6)} = 11.66$, $P = 0.0086$, post-hoc $P = 0.0134$ vs MAG1-low, $P = 0.0241$ vs control). Theoretically, The MMP-9/TIMP-1 complex is dissociated by the presence of SDS during the electrophoresis, resulting in no clear bands found at their expected positions. The activity of MMP-9 multimer (~220 kDa) and MMP-9/NGAL complex (~130 kDa) were only shown in one MAG1-high mice, and this was occurred at very low levels (Fig. 3).

3.4. An increase in the levels of GSK-3 concomitant with a decrease in pGSK-3

There is evidence that increasing Glycogen synthase kinase 3 (GSK-3) activity can induce MMP-9 expression, and both cooperate in the control of dendritic spine morphology (Kondratiuk et al., 2017). We evaluated cerebellar expression of GSK-3 to determine if it is correlated with elevated levels of MMP-9. Our results revealed increased total GSK-3 (α and β) levels in the MAG1-high mice compared to controls (Fig. 4A, for GSK-3α: $t (8) = 4.754$, $P = 0.0014$; for GSK-3β: $t (8) = 2.711$, $P = 0.0266$). GSK-3 protein levels do not directly indicate GSK-3 activity. The activity of GSK-3 is controlled by phosphorylation. Thus, an indirect way to explore GSK-3 activity is to investigate the phosphorylation of GSK-3 at serine-21 for GSK-3α and serine-9 for GSK-3β (Beurel et al., 2015). As shown in Fig. 4B, GSK-3β phosphorylation at serine-9 decreased significantly in MAG1-high mice ($t (8) = 3.141$, $P = 0.0138$), while GSK-3α phosphorylation at serine 21 showed a trend toward decrease ($t (8) = 1.993$, $P = 0.0814$).

### 3.5. Elevated cerebellar expression of MMP-9, especially in the purkinje cells

Since increased MMP-9 levels were only found in the MAG1-high mice, we immunostained brain sections of this group with anti-MMP-9 antibodies. Fig. 5A–C shows minimal staining in the granular, molecular, and Purkinje cell layers of uninfected control mice. In MAG1-high mice, there was an increase in MMP-9 staining, particularly in Purkinje layers (Fig. 5D–F). Intense staining of MMP-9 was observed in the cytoplasmic membranes and at the terminal branches of Purkinje cells, which were identified based on their location and distribution (Fig. 5D–E). Numerous MMP-9-positive structures in the granular and molecular layers appeared as dot-shaped or cytoplasmic membrane staining (Fig. 5E–F).

3.6. Elevated expression of MMP-9 associated with diminished perineuronal nets

MMP-9 is essential for regulating and organizing PNNs (Reinhard et al., 2015). To analyze the impact of increased MMP-9 expression, we investigated the cerebellar dispersion of PNNs by histochemical staining with the lectin WFA which binds to chondroitin sulfate in PNNs. In line with previous reports (Corvetti and Rossi, 2005), WFA staining was the most intense in the granular layer, which displayed a lattice-like labeling pattern, with patches of different intensity and pericellular nets around Golgi neurons (Fig. 6A). WFA staining was also observed in the terminal branches of Purkinje cells and the molecular layer (Fig. 6D–E). However, we found that MAG1-high mice had diminished WFA labeling (F) compared to controls, exhibiting reduced labeling in the granular layer, molecular layer, and around the cell bodies of Purkinje cells (Fig. 6I–J, and Supplementary Fig. 1). When we double-stained WFA with MMP-9 (Fig. 6A–C, F-H), we observed that they were co-localized but had antithetical associations (Fig. 6H). For instance, Purkinje cell bodies exhibited strong MMP-9 labeling but diminished PNNs (Fig. 6I). A similar association was also observed in the granular layer, where limited WFA staining is associated with intense MMP-9 staining (Fig. 6J).

The inverse relationship between MMP-9 and PNNs was further supported by analyzing their protein expression. We measured protein expressions of two components of PNNs, aggrecan and brevican, in the mouse cerebellum, and compared with that of MMP-9. Immunoblots using anti-aggrecan antibodies showed the presence of full-length aggrecan (approximately 350 kDa), while anti-brevican antibodies detected total brevican (around 145 kDa). The expression of aggrecan was significantly lower in MAG1-high mice than that in control mice, as shown in Fig. 6K ($t (9) = 3.192$, $P = 0.011$). There was a trend toward a negative correlation between aggrecan and MMP-9 in the cerebellum ($r = 0.56$, $P = 0.0719$, Fig. 6K). However, no significant difference was
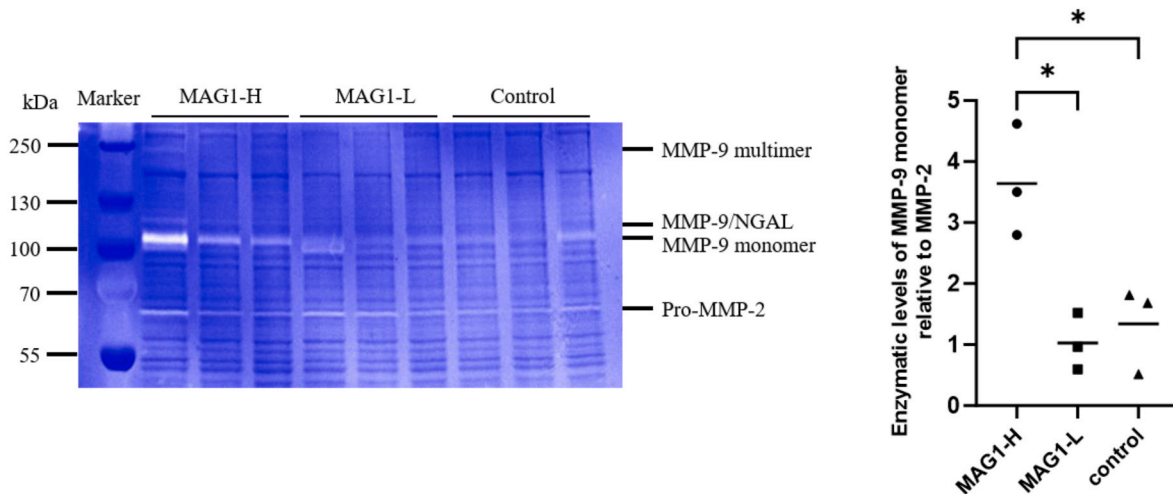
Fig. 3. Cyst-associated elevation of enzymatic activity of the MMP-9 monomer. Enzymatic levels of MMP-9 and MMP-2 were analyzed using gelatin-substrate zymography among MAG1-high, MAG1-low, and control mice (n = 3 per group). Each data point and means obtained by densitometry analysis of blots were shown. *p < 0.05 (one-way ANOVA followed by Bonferroni's correction for multiple comparisons).

A

B
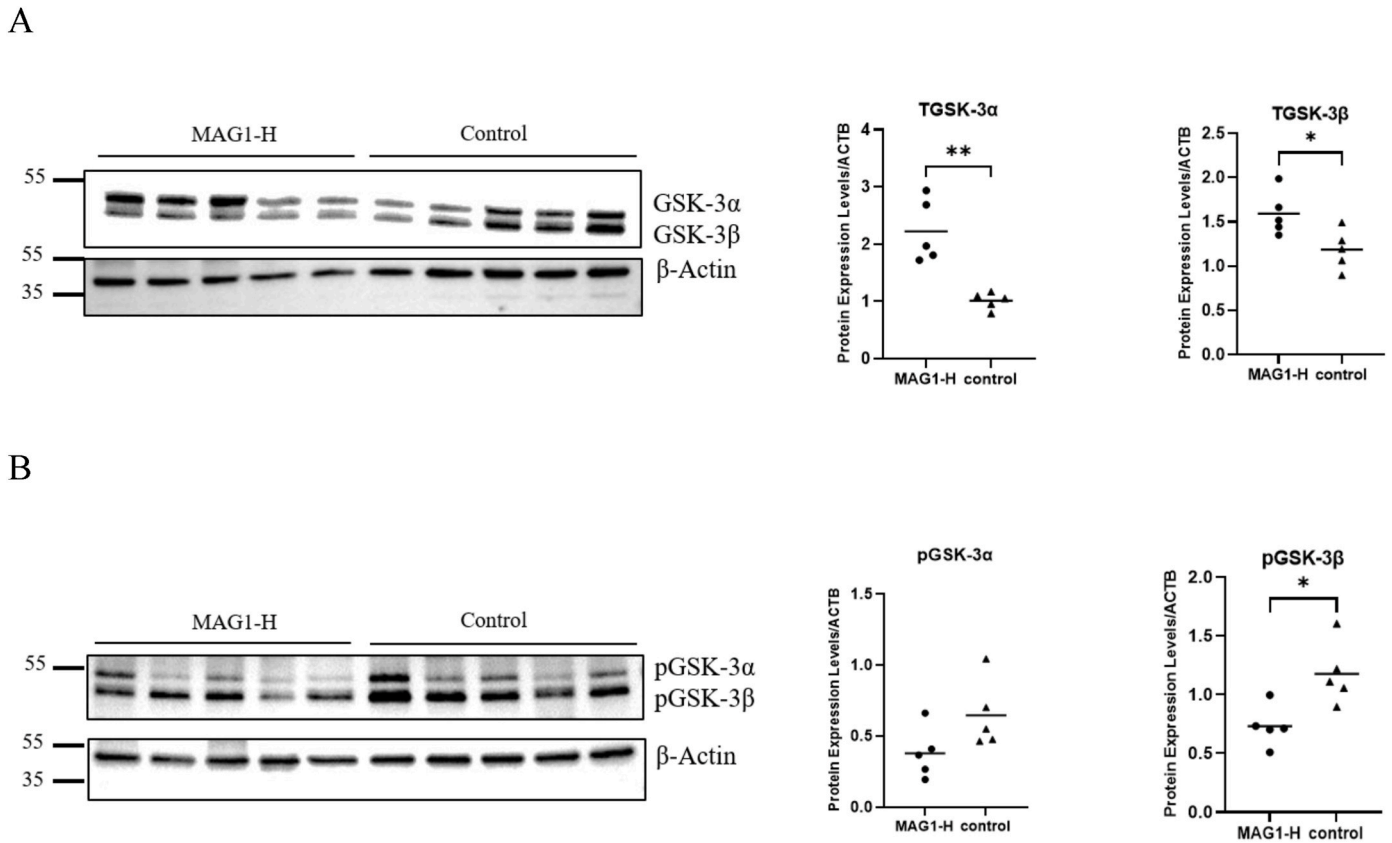
Fig. 4. Mice with a high burden of tissue cysts showed elevated levels of GSK-3 and reduced levels of pGSK-3. Western blot analysis of cerebellar protein extracts from MAG1-high or control mice probed with antibodies against GSK-3α/β (A) and pGSK-3αSer21/βSer9 (B). Each data point and means obtained by densitometry analysis of blots were shown. *p < 0.05, **p < 0.01 (unpaired *t*-test). N = 5 per group.

observed for brevican between the two groups (P = 0.635), and its expression was not associated with MMP-9 (P = 0.498, Fig. 6L).

### 3.7. Toxoplasma tissue cyst-associated elevation of synaptophysin co-localization with MMP-9

We evaluated the effect of diminished PNNs on cerebellar synaptophysin expression. Synaptophysin is the most studied presynaptic protein and an accurate index of neuronal synaptic density (Calhoun et al., 1996). We found that MAG1-high mice had a higher protein expression of synaptophysin than MAG1-low or control mice ($F_{(2, 6)}$ = 8.893, P = 0.0161, post-hoc P = 0.0232 vs MAG1-low, P = 0.0497 vs control, Fig. 7A). Consistent with the protein results, immunocytochemistry revealed an elevated synaptophysin level at the granular layer in MAG1-high mice compared to the uninfected controls (Fig. 7B&C). Synaptophysin reactivity was typically present in a punctate pattern indicative of synapses and alongside neuronal cell processes (Fig. 7D). Additionally, synaptophysin was detected in cell bodies as a granular cytoplasmic pattern. When double staining was performed between synaptophysin and MMP-9, we observed that MMP-9 expression was present in conjunction with synaptophysin throughout the cytoplasm and processes of neuronal cells (Fig. 7F). Colocalization analyses gave a Pearson's coefficient of 23 % (Mean ± SD: 0.23 ± 0.06) for the overall overlay of synaptophysin with MMP-9. No colocalization analysis was performed in the uninfected control mice due to minimal or absent staining.

4. Discussion

We investigated whether MMP-9 and PNN are involved in the neuropathology of *Toxoplasma* infection. In mice with a high parasite

burden, we demonstrated that MMP-9 expression was increased in brain tissue, specific neural cells, and peripheral circulation. There was a positive correlation between serum levels of MMP-9 and MAG1 antibody, a surrogate marker of tissue cysts in the brain (Xiao et al., 2013, 2021). MMP-9 elevation was accompanied by increased expression of its endogenous regulators, TIMP-1 and NGAL. We also documented the elevation of GSK-3α/β, together with suppression in inhibitory GSK-3α/β (Ser-21/Ser-9) phosphorylation. There was a notable association between increased MMP-9 expression and the loss of PNNs, accompanied by an increase in synaptophysin expression. The association was supported by a negative trend between MMP-9 and aggrecan expression, a core component of PNNs. Our results suggest that tissue cysts, the hallmark of chronic *Toxoplasma* infection, are crucial for the increase in MMP-9 expression and the resulting degradation of regulators essential in synaptic plasticity. Since synaptic plasticity is the primary mechanism for learning and memory (Ramirez and Arbuckle, 2016), our research sheds light on mechanisms underlying cognitive impairments associated with *Toxoplasma* infection, as well as the increased odds of *Toxoplasma* exposure observed in brain disorders.

We demonstrated increased levels of MMP-9 complexes (MMP9/TIMP-1, MMP9/NGAL) and related monomers (MMP-9, TIMP-1, and NGAL) in the cerebellum of MAG1-high mice when analyzed under non-reducing and reducing conditions. The results of gelatin zymography showed increased enzyme levels of monomeric MMP-9. The increase in MMP-9/NGAL complex indicates that MMP-9 activity is more durable due to NGAL protection, while the enhanced MMP-9/TIMP-1 complex supports the protective role of TIMP-1. Previous studies have reported significant elevations or correlations between levels of MMP-9, TIMP-1, and MMP-9 complexes in a range of neuropsychiatric conditions, including Alzheimer's Disease, mild cognitive impairment, stroke, and schizophrenia (Chang et al., 2011; Domenici et al., 2010; Lorenzl et al.,
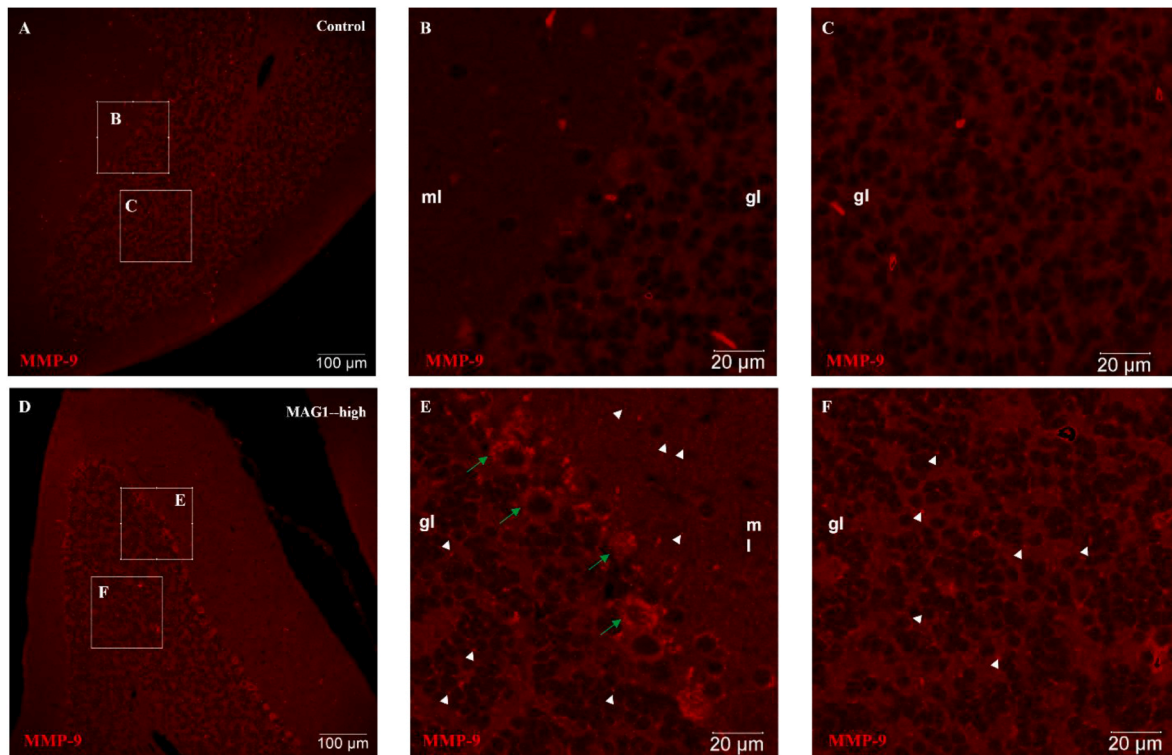
Fig. 5. Elevated cerebellar expression of MMP-9, particularly in the Purkinje cells, of MAG1-high mice. (A–C) Little MMP-9-positive staining was found in the granular, molecular, and Purkinje cell layers of uninfected control mice. (D–F) There was an increased cerebellar MMP-9 staining in the MAG1-high mice. Intense staining of MMP-9 was observed in the cytoplasmic membranes and at the terminal branches of Purkinje cells (green arrow, E). Numerous MMP-9-positive structures in the granular and molecular layers appeared as dot-shaped or cytoplasmic membrane staining (white arrowhead, Fig. 5E–F). Scale bars are indicated. gl: granular layer; ml: molecular layer.

2003; Rosell et al., 2006; Wei et al., 2016). Our findings offer a mechanical explanation for the link between *Toxoplasma* and multiple brain disorders. Studies reported that miR-132 can regulate MMP-9 mRNA via binding to its 3′UTR in neurons (Jasinska et al., 2016). Our previous study revealed that chronic *Toxoplasma* infection reduces miR-132 expression in multiple mouse brain regions, including the cerebellum (Li et al., 2015), possibly accounting for the elevated MMP-9 expression observed here.

GSK-3 is a crucial player in numerous signaling pathways and exhibits high pleiotropy by phosphorylating over a hundred substrates that contribute to essential functions such as metabolism, cell structure, and gene expression. Studies suggest that GSK-3 is involved in MMP-9 expression and has a joint role in regulating the shape of dendritic spines (Kondratiuk et al., 2017). In MAG1-high mice with MMP-9 elevation, we observed the activation of GSK-3α/β, concomitant with the suppression of inhibitory GSK-3α/β phosphorylation. A previous study found that chronic *Toxoplasma* infection decreases dendritic complexity and spine density (Parlog et al., 2014). Kondratiuk et al. found that MMP-9 is important for initiating the Akt-GSK-3 cascade in neurons (Kondratiuk et al., 2017), pathways known to be altered in *Toxoplasma* infection (Wang et al., 2010). Moreover, increased GSK-3 activity is reported to contribute to the pathogenesis of neurodegenerative diseases like AD (Hernandez et al., 2013) and bipolar disorder (Beaulieu et al., 2004).

Perineuronal nets are structures that surround a subset of fast-spiking interneurons implicated in learning and memory. In MAG1-high mice, we observed reduced PNNs and decreased expression of aggrecan in the cerebellum. Two studies have shown that PNNs in the cerebellum play a crucial role in eyeblink conditioning, a form of cerebellar motor learning. The first study (Hirono et al., 2018) found that depleting PNNs can increase the release of GABA from presynaptic Purkinje cell terminals, resulting in a delay during eyeblink

conditioning. The second study (Carulli et al., 2020) demonstrated that intact PNNs are necessary for memory retention during eyeblink conditioning. Another study reported that the loss of aggrecan can ablate the PNN structure and cause a shift in parvalbumin-expressing inhibitory interneurons toward a high plasticity state (Rowlands et al., 2018). The degradation of PNN was notably associated with increased expression of MMP-9. This is consistent with previous research on Fragile X Syndrome, HIV-infected brain, and patients with multiple sclerosis (Bozzelli et al., 2020; Gray et al., 2008; Wen et al., 2018a). Additionally, there was a negative tendency between aggrecan and MMP-9 expression. Overall, our findings suggest that the increased expression of MMP-9 may have contributed to the reduced expression of aggrecan and PNNs. Since PNNs play a crucial role in memory, neuroprotection, plasticity, and various brain disorders (Wen et al., 2018b), their degradation could contribute to *Toxoplasma*-associated neuropsychiatric disorders including learning and memory impairments.

There is usually a rise in network activity when PNNs are reduced, possibly due to a decrease in inhibitory activity (Fawcett et al., 2022). In line with this, we observed a significant increase in synaptophysin expression in MAG1-high mice with reduced PNNs. Synaptophysin modulates the efficiency of the synaptic vesicle cycle (Valtorta et al., 2004). Research has shown that overexpression of synaptophysin can lead to an increase in glutamate release (Alder et al., 1992), which has been observed in mice infected with *Toxoplasma* (David et al., 2016; Li et al., 2018). The abnormal expression of synaptophysin has been associated with several brain disorders (de Wilde et al., 2016; Osimo et al., 2019). For example, patients with AD have been found to have higher rates of synaptophysin-bearing microvesicles in their cerebrospinal fluid (Utz et al., 2021). Moreover, synaptophysin has been suggested as a reliable marker of axonal damage in the CNS in demyelinating and neuroinflammatory conditions (Gudi et al., 2017).

*Toxoplasma* infections in humans can be prevented through
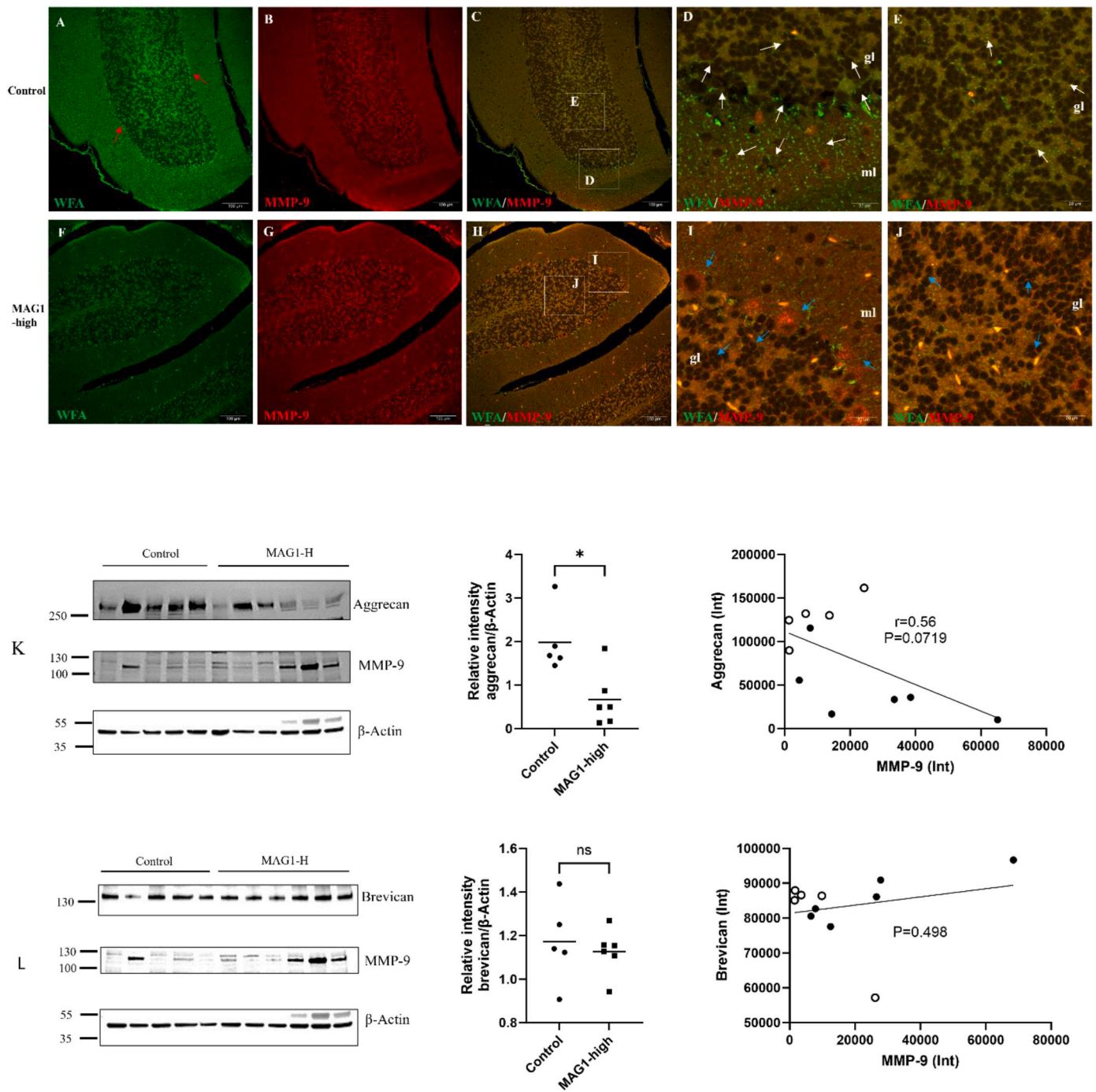
Fig. 6. **A diminished WFA staining was associated with MMP-9 expression in MAG1-high mice**. The WFA staining showed a lattice-like pattern in the granular layer and was present in the terminal branches of Purkinje cells (red arrows), as shown in the control mice (A). The white arrows indicate the presence of pericellular nets (green) surrounding Golgi neurons located in the granular layer, in the proximal dendrites of interneurons in the molecular layer, and at the terminal branches of Purkinje cells (D–E). In contrast, MAG1-high mice had diminished WFA labeling in the cerebellar cortex (F). Double-labeling of WFA and MMP-9 (A-C, F–H) showed that MMP-9 expression was associated with diminished WFA staining (H). The blue arrows point to MMP-9 staining (red) occurring in the granular layer and the Purkinje cell bodies (I–J). Scale bar = 100 μm or 20 μm. gl: granular layer; ml: molecular layer. Protein extracts from cerebellar homogenates of MAG1-high and control mice were probed with antibodies against aggrecan (K) and brevican (L), alongside MMP-9 and β-actin. Each data point and means obtained by densitometry analysis of blots were shown. Correlations between PNN protein expression and MMP-9 were evaluated. Control (n = 5, circles); MAG1-high (n = 6, black dots). Statistically significant differences were determined by unpaired t-test or Pearson's correlation analysis. *p < 0.05, ns: not significant.

environmental modifications such as water purification, safe handling of infectious cat feces, and the proper cooking of dietary meat (Smith et al., 2021). There is also interest in developing improved methods for preventing *Toxoplasma* infections through vaccines (Zhang et al., 2023) or treatments with novel anti-protozoal agents (Doggett et al., 2012; Xiao et al., 2018a, 2023). Establishing a linkage between *Toxoplasma*

infection and brain disorders associated with PNN degradation might lead to new methods for preventing and treating these diseases. The present study shows that *Toxoplasma* tissue cysts are associated with increased levels of MMP-9, TIMP-1, NGAL, GSK-3α/β, and synaptophysin, as well as a loss of PNNs. Further research using pharmacological or genetic approaches is needed to determine the functional role of
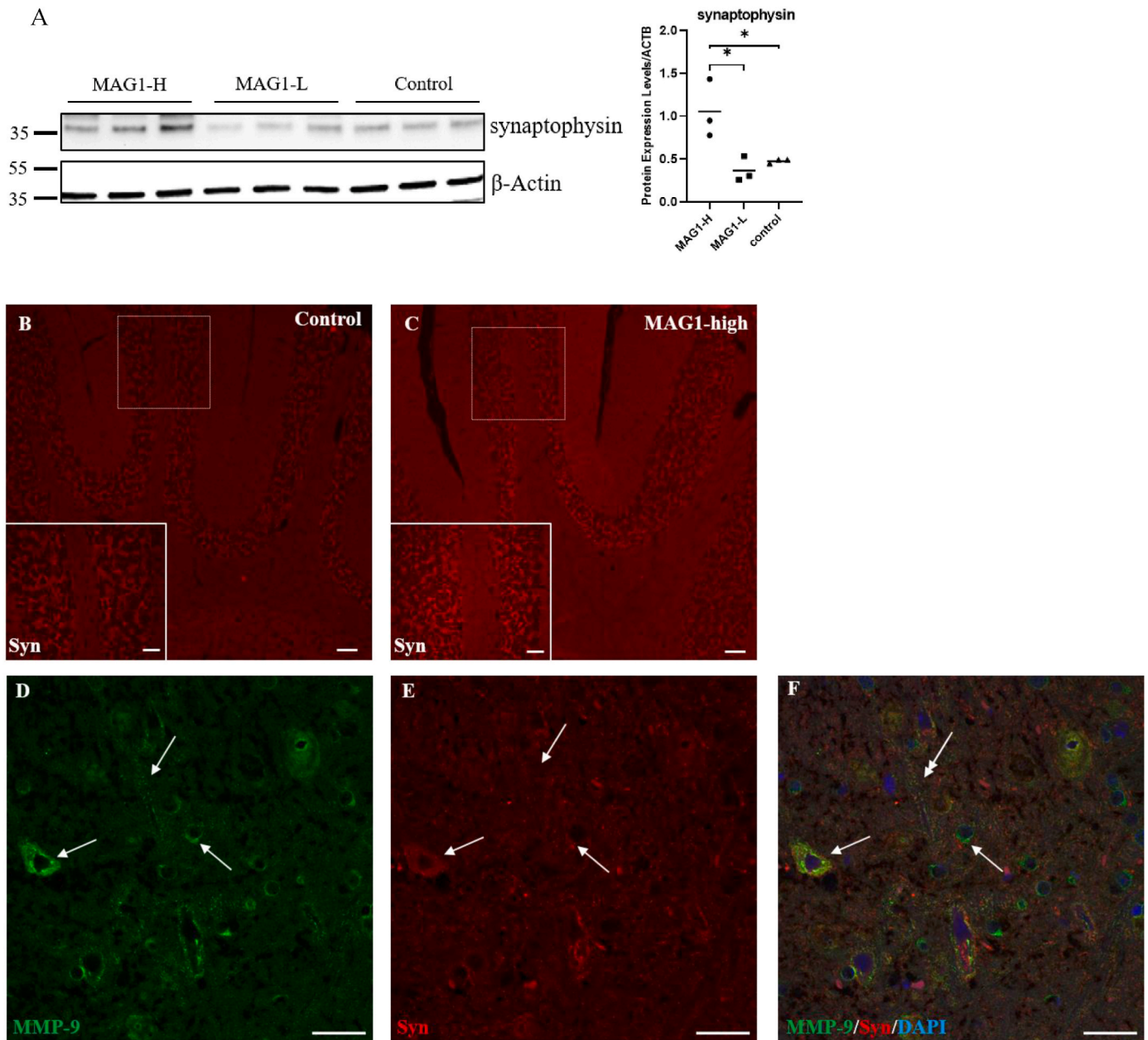
Fig. 7. Mice with a high burden of tissue cysts exhibited increased synaptophysin expression in the cerebellum, located adjacent to MMP-9. (A) Western blot analysis of cerebellar protein extracts from MAG1-high, MAG1-low, or control mice probed with antibodies against synaptophysin. Each data point and means obtained by densitometry analysis of blots were shown. Compared to the uninfected control (B), synaptophysin levels in the granular layer were elevated in MAG1-high mice (C). The white boxes inserted are at ×40 Magnification. (D–F) Confocal images show the proximity of the staining for MMP-9 and synaptophysin throughout the cytoplasm and processes of neuronal cells (white arrows). DAPI was used to identify nuclei (blue). Scale bar, 200 μm or 100 μm (inserts). *p < 0.05 (one-way ANOVA followed by Bonferroni's correction for multiple comparisons). Syn: synaptophysin.

these molecular elements in the context of chronic toxoplasmosis.

CRediT authorship contribution statement

Jianchun Xiao: Conceptualization, Formal analysis, Investigation, Methodology, Project administration, Supervision, Writing – original draft, Writing – review & editing. **Jing Huang:** Investigation. **Robert H. Yolken:** Conceptualization, Funding acquisition, Writing – review & editing.

Declaration of competing interest

None

Data availability

Data will be made available on request.

Appendix A. Supplementary data

Supplementary data to this article can be found online at https://doi.

org/10.1016/j.bbih.2024.100728.

References

Alder, J., Lu, B., Valtorta, F., Greengard, P., Poo, M.M., 1992. Calcium-dependent transmitter secretion reconstituted in Xenopus oocytes: requirement for synaptophysin. Science 257, 657–661.

Beaulieu, J.M., Sotnikova, T.D., Yao, W.D., Kockeritz, L., Woodgett, J.R., Gainetdinov, R. R., Caron, M.G., 2004. Lithium antagonizes dopamine-dependent behaviors mediated by an AKT/glycogen synthase kinase 3 signaling cascade. Proc Natl Acad Sci U S A 101, 5099–5104.

Bertolotto, A., Manzardo, E., Guglielmone, R., 1996. Immunohistochemical mapping of perineuronal nets containing chondroitin unsulfated proteoglycan in the rat central nervous system. Cell Tissue Res. 283, 283–295.

Beurel, E., Grieco, S.F., Jope, R.S., 2015. Glycogen synthase kinase-3 (GSK3): regulation, actions, and diseases. Pharmacol. Ther. 148, 114–131.

Bolte, S., Cordelieres, F.P., 2006. A guided tour into subcellular colocalization analysis in light microscopy. J Microsc 224, 213–232.

Brkic, M., Balusu, S., Libert, C., Vandenbroucke, R.E., 2015. Friends or foes: matrix metalloproteinases and their multifaceted roles in neurodegenerative diseases. Mediat. Inflamm. 2015, 620581.

Bruschi, F., Pinto, B., 2013. The significance of matrix metalloproteinases in parasitic infections involving the central nervous system. Pathogens 2, 105–129.

Calhoun, M.E., Jucker, M., Martin, L.J., Thinakaran, G., Price, D.L., Mouton, P.R., 1996. Comparative evaluation of synaptophysin-based methods for quantification of synapses. J. Neurocytol. 25, 821–828.

Carulli, D., Broersen, R., de Winter, F., Muir, E.M., Meskovic, M., de Waal, M., de Vries, S., Boele, H.J., Canto, C.B., De Zeeuw, C.I., Verhaagen, J., 2020. Cerebellar plasticity and associative memories are controlled by perineuronal nets. Proc Natl Acad Sci U S A 117, 6855–6865.

Chang, S.H., Chiang, S.Y., Chiu, C.C., Tsai, C.C., Tsai, H.H., Huang, C.Y., Hsu, T.C., Tzang, B.S., 2011. Expression of anti-cardiolipin antibodies and inflammatory associated factors in patients with schizophrenia. Psychiatr. Res. 187, 341–346.

Corvetti, L., Rossi, F., 2005. Degradation of chondroitin sulfate proteoglycans induces sprouting of intact purkinje axons in the cerebellum of the adult rat. J. Neurosci. 25, 7150–7158.

David, C.N., Frias, E.S., Szu, J.I., Vieira, P.A., Hubbard, J.A., Lovelace, J., Michael, M., Worth, D., McGovern, K.E., Ethell, I.M., Stanley, B.G., Korzus, E., Fiacco, T.A., Binder, D.K., Wilson, E.H., 2016. GLT-1-Dependent disruption of CNS glutamate homeostasis and neuronal function by the Protozoan parasite Toxoplasma gondii. PLoS Pathog. 12, e1005643.

de Wilde, M.C., Overk, C.R., Sijben, J.W., Masliah, E., 2016. Meta-analysis of synaptic pathology in Alzheimer's disease reveals selective molecular vesicular machinery vulnerability. Alzheimers Dement 12, 633–644.

DeLeon-Pennell, K.Y., Meschiari, C.A., Jung, M., Lindsey, M.L., 2017. Matrix metalloproteinases in myocardial infarction and heart failure. Prog Mol Biol Transl Sci 147, 75–100.

Doggett, J.S., Nilsen, A., Forquer, I., Wegmann, K.W., Jones-Brando, L., Yolken, R.H., Bordon, C., Charman, S.A., Katneni, K., Schultz, T., Burrows, J.N., D.J., Meunier, B., Carruthers, V.B., Riscoe, M.K., 2012. Endochin-like quinolones are highly efficacious against acute and latent experimental toxoplasmosis. Proc Natl Acad Sci U S A 109, 15936–15941.

Domenici, E., Wille, D.R., Tozzi, F., Prokopenko, I., Miller, S., McKeown, A., Brittain, C., Rujescu, D., Giegling, I., Turck, C.W., Holsboer, F., Bullmore, E.T., Middleton, L., Merlo-Pich, E., Alexander, R.C., Muglia, P., 2010. Plasma protein biomarkers for depression and schizophrenia by multi analyte profiling of case-control collections. PLoS One 5, e9166.

Dzwonek, J., Rylski, M., Kaczmarek, L., 2004. Matrix metalloproteinases and their endogenous inhibitors in neuronal physiology of the adult brain. FEBS Lett. 567, 129–135.

Fawcett, J.W., Fyhn, M., Jendelova, P., Kwok, J.C.F., Ruzicka, J., Sorg, B.A., 2022. The extracellular matrix and perineuronal nets in memory. Mol. Psychiatr. 27, 3192–3203.

Ferguson, D.J., Parmley, S.F., 2002. Toxoplasma gondii MAG1 protein expression. Trends Parasitol. 18, 482.

Giamanco, K.A., Morawski, M., Matthews, R.T., 2010. Perineuronal net formation and structure in aggrecan knockout mice. Neuroscience 170, 1314–1327.

Gray, E., Thomas, T.L., Betmouni, S., Scolding, N., Love, S., 2008. Elevated matrix metalloproteinase-9 and degradation of perineuronal nets in cerebrocortical multiple sclerosis plaques. J. Neuropathol. Exp. Neurol. 67, 888–899.

Gudi, V., Gai, L., Herder, V., Tejedor, L.S., Kipp, M., Amor, S., Suhs, K.W., Hansmann, F., Beineke, A., Baumgartner, W., Stangel, M., Skripuletz, T., 2017. Synaptophysin is a reliable marker for axonal damage. J. Neuropathol. Exp. Neurol. 76, 109–125.

Hernandez, F., Lucas, J.J., Avila, J., 2013. GSK3 and tau: two convergence points in Alzheimer's disease. J Alzheimers Dis 33 (Suppl. 1), S141–S144.

Hirono, M., Watanabe, S., Karube, F., Fujiyama, F., Kawahara, S., Nagao, S., Yanagawa, Y., Misonou, H., 2018. Perineuronal nets in the deep cerebellar nuclei regulate GABAergic transmission and delay eyeblink conditioning. J. Neurosci. 38, 6130–6144.

Jasinska, M., Milek, J., Cymerman, I.A., Leski, S., Kaczmarek, L., Dziembowska, M., 2016. miR-132 regulates dendritic spine structure by direct targeting of matrix metalloproteinase 9 mRNA. Mol. Neurobiol. 53, 4701–4712.

Kannan, G., Pletnikov, M.V., 2012. Toxoplasma gondii and cognitive deficits in schizophrenia: an animal model perspective. Schizophr. Bull. 38, 1155–1161.

Kittaka, S., Hasegawa, S., Ito, Y., Ohbuchi, N., Suzuki, E., Kawano, S., Aoki, Y., Nakatsuka, K., Kudo, K., Wakiguchi, H., Kajimoto, M., Matsushige, T., Ichiyama, T., 2014. Serum levels of matrix metalloproteinase-9 and tissue inhibitor of metalloproteinases-1 in human herpesvirus-6-infected infants with or without febrile seizures. J. Infect. Chemother. 20, 716–721.

Kondratiuk, I., Leski, S., Urbanska, M., Biecek, P., Devijver, H., Lechat, B., Van Leuven, F., Kaczmarek, L., Jaworski, T., 2017. GSK-3 beta and MMP-9 cooperate in the control of dendritic spine morphology. Mol. Neurobiol. 54, 200–211.

Leppert, D., Leib, S.L., Grygar, C., Miller, K.M., Schaad, U.B., Hollander, G.A., 2000. Matrix metalloproteinase (MMP)-8 and MMP-9 in cerebrospinal fluid during bacterial meningitis: association with blood-brain barrier damage and neurological sequelae. Clin. Infect. Dis. 31, 80–84.

Li, Y., Severance, E.G., Viscidi, R.P., Yolken, R.H., Xiao, J., 2019. Persistent Toxoplasma infection of the brain induced neurodegeneration associated with activation of complement and microglia. Infect. Immun. 87.

Li, Y., Viscidi, R.P., Kannan, G., McFarland, R., Pletnikov, M.V., Severance, E.G., Yolken, R.H., Xiao, J., 2018. Chronic Toxoplasma gondii infection induces anti-N-Methyl-d-Aspartate receptor autoantibodies and associated behavioral changes and neuropathology. Infect. Immun. 86.

Li, Y.E., Kannan, G., Pletnikov, M.V., Yolken, R.H., Xiao, J., 2015. Chronic infection of Toxoplasma gondii downregulates miR-132 expression in multiple brain regions in a sex-dependent manner. Parasitology 142, 623–632.

Lorenzl, S., Albers, D.S., Relkin, N., Ngyuen, T., Hilgenberg, S.L., Chirichigno, J., Cudkowicz, M.E., Beal, M.F., 2003. Increased plasma levels of matrix metalloproteinase-9 in patients with Alzheimer's disease. Neurochem. Int. 43, 191–196.

Lu, C.Y., Lai, S.C., 2013. Matrix metalloproteinase-2 and -9 lead to fibronectin degradation in astroglia infected with Toxoplasma gondii. Acta Trop. 125, 320–329.

Nicholson, C., Sykova, E., 1998. Extracellular space structure revealed by diffusion analysis. Trends Neurosci. 21, 207–215.

Olson, M.W., Bernardo, M.M., Pietila, M., Gervasi, D.C., Toth, M., Kotra, L.P., Massova, I., Mobashery, S., Fridman, R., 2000. Characterization of the monomeric and dimeric forms of latent and active matrix metalloproteinase-9. Differential rates for activation by stromelysin 1. J. Biol. Chem. 275, 2661–2668.

Osimo, E.F., Beck, K., Reis Marques, T., Howes, O.D., 2019. Synaptic loss in schizophrenia: a meta-analysis and systematic review of synaptic protein and mRNA measures. Mol. Psychiatr. 24, 549–561.

Park, K.P., Rosell, A., Foerch, C., Xing, C., Kim, W.J., Lee, S., Opdenakker, G., Furie, K.L., Lo, E.H., 2009. Plasma and brain matrix metalloproteinase-9 after acute focal cerebral ischemia in rats. Stroke 40, 2836–2842.

Parlog, A., Harsan, L.A., Zagrebelsky, M., Weller, M., von Elverfeldt, D., Mawrin, C., Korte, M., Dunay, I.R., 2014. Chronic murine toxoplasmosis is defined by subtle changes in neuronal connectivity. Dis Model Mech 7, 459–469.

Phillips, J.R., Hewedi, D.H., Eissa, A.M., Moustafa, A.A., 2015. The cerebellum and psychiatric disorders. Front. Public Health 3, 66.

Pollock, E., Everest, M., Brown, A., Poulter, M.O., 2014. Metalloproteinase inhibition prevents inhibitory synapse reorganization and seizure genesis. Neurobiol. Dis. 70, 21–31.

Ramirez, A., Arbuckle, M.R., 2016. Synaptic plasticity: the role of learning and unlearning in addiction and beyond. Biol. Psychiatr. 80, e73–e75.

Ramsey, K.H., Sigar, I.M., Schripsema, J.H., Shaba, N., Cohoon, K.P., 2005. Expression of matrix metalloproteinases subsequent to urogenital Chlamydia muridarum infection of mice. Infect. Immun. 73, 6962–6973.

Reinhard, S.M., Razak, K., Ethell, I.M., 2015. A delicate balance: role of MMP-9 in brain development and pathophysiology of neurodevelopmental disorders. Front. Cell. Neurosci. 9, 280.

Rosell, A., Ortega-Aznar, A., Alvarez-Sabin, J., Fernandez-Cadenas, I., Ribo, M., Molina, C.A., Lo, E.H., Montaner, J., 2006. Increased brain expression of matrix metalloproteinase-9 after ischemic and hemorrhagic human stroke. Stroke 37, 1399–1406.

Rowlands, D., Lensjo, K.K., Dinh, T., Yang, S., Andrews, M.R., Hafting, T., Fyhn, M., Fawcett, J.W., Dick, G., 2018. Aggrecan directs extracellular matrix-mediated neuronal plasticity. J. Neurosci. 38, 10102–10113.

Smith, N.C., Goulart, C., Hayward, J.A., Kupz, A., Miller, C.M., van Dooren, G.G., 2021. Control of human toxoplasmosis. Int. J. Parasitol. 51, 95–121.

Sorg, B.A., Berretta, S., Blacktop, J.M., Fawcett, J.W., Kitagawa, H., Kwok, J.C., Miquel, M., 2016. Casting a wide net: role of perineuronal nets in neural plasticity. J. Neurosci. 36, 11459–11468.

Spann, M.N., Sourander, A., Surcel, H.M., Hinkka-Yli-Salomaki, S., Brown, A.S., 2017. Prenatal toxoplasmosis antibody and childhood autism. Autism Res. 10, 769–777.

Testa, D., Prochiantz, A., Di Nardo, A.A., 2019. Perineuronal nets in brain physiology and disease. Semin. Cell Dev. Biol. 89, 125–135.

Utz, J., Berner, J., Munoz, L.E., Oberstein, T.J., Kornhuber, J., Herrmann, M., Maler, J. M., Spitzer, P., 2021. Cerebrospinal fluid of patients with Alzheimer's disease contains increased percentages of synaptophysin-bearing microvesicles. Front. Aging Neurosci. 13, 682115.

Vafadari, B., Salamian, A., Kaczmarek, L., 2016. MMP-9 in translation: from molecule to brain physiology, pathology, and therapy. J. Neurochem. 139 (Suppl. 2), 91–114.

Valtorta, F., Pennuto, M., Bonanomi, D., Benfenati, F., 2004. Synaptophysin: leading actor or walk-on role in synaptic vesicle exocytosis? Bioessays 26, 445–453.

Wang, Y., Weiss, L.M., Orlofsky, A., 2010. Coordinate control of host centrosome position, organelle distribution, and migratory response by Toxoplasma gondii via host mTORC2. J. Biol. Chem. 285, 15611–15618.

Wei, T., Zhang, H., Cetin, N., Miller, E., Moak, T., Suen, J.Y., Richter, G.T., 2016. Elevated expression of matrix metalloproteinase-9 not matrix metalloproteinase-2

contributes to progression of extracranial arteriovenous malformation. Sci. Rep. 6, 24378.

Wen, T.H., Afroz, S., Reinhard, S.M., Palacios, A.R., Tapia, K., Binder, D.K., Razak, K.A., Ethell, I.M., 2018a. Genetic reduction of matrix metalloproteinase-9 promotes formation of perineuronal nets around parvalbumin-expressing interneurons and normalizes auditory cortex responses in developing Fmr1 knock-out mice. Cerebr. Cortex 28, 3951–3964.

Wen, T.H., Binder, D.K., Ethell, I.M., Razak, K.A., 2018b. The perineuronal 'safety' net? Perineuronal net abnormalities in neurological disorders. Front. Mol. Neurosci. 11, 270.

Xiao, J., Bhondoekhan, F., Seaberg, E.C., Yang, O., Stosor, V., Margolick, J.B., Yolken, R. H., Viscidi, R.P., 2021. Serological responses to Toxoplasma gondii and matrix antigen 1 predict the risk of subsequent toxoplasmic encephalitis in people living with human immunodeficiency virus (HIV). Clin. Infect. Dis. 73, e2270–e2277.

Xiao, J., Li, Y., Prandovszky, E., Kannan, G., Viscidi, R.P., Pletnikov, M.V., Yolken, R.H., 2016. Behavioral abnormalities in a mouse model of chronic toxoplasmosis are associated with MAG1 antibody levels and cyst burden. PLoS Negl Trop Dis 10, e0004674.

Xiao, J., Li, Y., Rowley, T., Huang, J., Yolken, R.H., Viscidi, R.P., 2023. Immunotherapy targeting the PD-1 pathway alleviates neuroinflammation caused by chronic Toxoplasma infection. Sci. Rep. 13, 1288.

Xiao, J., Li, Y., Yolken, R.H., Viscidi, R.P., 2018a. PD-1 immune checkpoint blockade promotes brain leukocyte infiltration and diminishes cyst burden in a mouse model of Toxoplasma infection. J. Neuroimmunol. 319, 55–62.

Xiao, J., Prandovszky, E., Kannan, G., Pletnikov, M.V., Dickerson, F., Severance, E.G., Yolken, R.H., 2018b. Toxoplasma gondii: biological parameters of the connection to schizophrenia. Schizophr. Bull. 44, 983–992.

Xiao, J., Savonenko, A., Yolken, R.H., 2022. Strain-specific pre-existing immunity: a key to understanding the role of chronic Toxoplasma infection in cognition and Alzheimer's diseases? Neurosci. Biobehav. Rev. 137, 104660.

Xiao, J., Viscidi, R.P., Kannan, G., Pletnikov, M.V., Li, Y., Severance, E.G., Yolken, R.H., Delhaes, L., 2013. The Toxoplasma MAG1 peptides induce sex-based humoral immune response in mice and distinguish active from chronic human infection. Microb. Infect. 15, 74–83.

Zhang, X., Yuan, H., Mahmmod, Y.S., Yang, Z., Zhao, M., Song, Y., Luo, S., Zhang, X.X., Yuan, Z.G., 2023. Insight into the current Toxoplasma gondii DNA vaccine: a review article. Expert Rev. Vaccines 22, 66–89.